



Electrochemically reductive dechlorination of 2,4,6-trichlorophenol on palladium loaded titanium cathode modified with graphene/polymeric pyrrole-sodium dodecyl benzene sulfonate

Zhirong Sun^{a,*}, Jinwei Zhang^a, Xueyun Wang^a, Xiang Hu^{b,*}

^aNational Engineering Laboratory for Advanced Municipal Wastewater Treatment and Reuse Technology, Beijing University of Technology, Beijing 100124, China, Tel. +86 10 67393533, Fax +86 10 67391983, email: zrsun@bjut.edu.cn (Z. Sun), zjwzhang@sina.com (J. Zhang), wangxy@bjut.edu.cn (X. Wang)

^bCollege of Chemical Engineering, Beijing University of Chemical Technology, Beijing 100029, China, Tel. +86 10 64427356, Fax +86 10 84718932, email: huxiang99@163.com (X. Hu)

Received 12 February 2017; Accepted 20 August 2017

ABSTRACT

Graphene (Gr)/polymeric pyrrole-sodium dodecyl benzene sulfonate (PPy-SDBS) were used to modify the palladium loaded titanium electrode. The palladium/graphene/polymeric pyrrole-sodium dodecyl benzene sulfonate/titanium (Pd/Gr/PPy-SDBS/Ti) electrode was successfully prepared by the simple drop-casting/electrodeposition process. The Pd/Gr/PPy-SDBS/Ti electrode showed high electrochemical activity in the application of the electrochemically reductive dechlorination of 2,4,6-trichlorophenol (2,4,6-TCP) in aqueous solution. The influence factors of dechlorination including dechlorination current and initial pH value were studied and the optimum dechlorination current and initial pH value within the investigated range were 5 mA and 2.3, respectively. Under these conditions, 100 mg L⁻¹ 2,4,6-TCP could be removed and dechlorinated completely within 80 min, and the current efficiency could reach 36%. The main final product of 2,4,6-TCP was phenol and the dechlorination pathways were studied according to the intermediate products detected by HPLC. The dechlorination reaction of 2,4,6-TCP fitted well to the pseudo-first-order kinetics. The effect of temperature on 2,4,6-TCP dechlorination and the stability of the prepared electrode were also investigated.

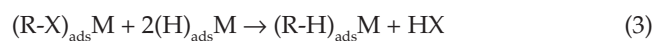
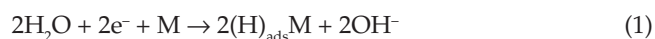
Keywords: Palladium/graphene/polymeric pyrrole-sodium dodecyl benzene sulfonate/titanium electrode; Graphene; 2,4,6-trichlorophenol; Electrochemically reductive dechlorination

1. Introduction

Chlorophenols (CPs), are important industrial organic compounds and widely used in pesticides, herbicides, fungicides and preservatives. But they are also common water contaminants, which have been attracted increasing interests due to their carcinogenic characteristics and persistence in natural environments [1–3]. The United States Environmental Protection Agency (USEPA) have listed some of them as priority pollutants [4,5]. Therefore, it is of vital importance to take measures to remove CPs from the environment.

In recent decades, many treatment techniques for the removal of chlorinated organic compounds, such as adsorption [6,7], advanced oxidation process [8] and biodegradation [9,10], have been developed. Recently, electrochemically reductive dechlorination has been developed and considered to be a kind of promising treatment approach for CPs dechlorination due to its various advantages including rapid reaction rate, mild reaction conditions, low facilities investment and the absence of secondary pollution [11,12]. The mechanism of electrochemically reductive dechlorination can be described as electrocatalytic hydrogenolysis (ECH) [13–15]. It involves several steps of reaction as described in Eqs. (1)–(4).

*Corresponding author.



where M, $(\text{H})_{\text{ads}}\text{M}$ and $(\text{R-X})_{\text{ads}}\text{M}$ represent electrode surface, adsorbed hydrogen on electrode surface and the adsorbed organic substrate on electrode surface, respectively. In this process, water is electrolyzed and the generated hydrogen atoms are adsorbed on the surface of electrode (H_{ads}) together with the chlorinated organic pollutants. Then the H_{ads} attack chlorine atoms adsorbed on the electrode surface, which results in the cleavage of carbon-halogen bond and the addition of hydrogen. Thus, chlorinated organic pollutants are dechlorinated. During this process, side reaction of hydrogen evolution reaction (HER) will occur inevitably, which is influenced by the reaction conditions and the electrochemical characteristics of the electrode.

In electrochemically reductive reaction, the electrode material has a significant influence on dechlorination performance [16–18]. Therefore, it is of vital importance to search for a suitable electrode material. Titanium (Ti) is usually selected as the substrate material of electrode for its good stability [19]. Noble metal catalyst palladium (Pd) is an effective dechlorination catalyst. It has been extensively used in CPs dechlorination because of the remarkable capacity for hydrogen storage [20,21]. However, the exorbitant price of Pd restricts its large-scale application [22]. Enhancing the specific surface area of Pd catalyst is an effective method to reduce its consumption. Therefore, many researchers attempted to support catalyst on different substrate materials or add middle layers to improve the specific surface area of the catalyst [23,24]. Graphene (Gr) with a two-dimensional (2D) monolayer of sp^2 -hybridized carbon atoms shows outstanding properties [25–28], such as very large surface area, extraordinary electronic transport properties, excellent thermal conductivity and superior mechanical property, which has attracted more and more attentions.

In the present work, aiming at making full use of Pd catalyst to improve the electrocatalytic performance of the electrode, graphene/polymeric pyrrole-sodium dodecyl benzene sulfonate (Gr/PPy-SDBS) were introduced to modify the electrode and Pd particles were electrodeposited on the electrode surface. The prepared palladium/graphene/polymeric pyrrole-sodium dodecyl benzene sulfonate/titanium (Pd/Gr/PPy-SDBS/Ti) electrode had high electrocatalytic activity. The characterizations of the electrode were investigated. 2,4,6-trichlorophenol (2,4,6-TCP) was selected as model compound to test the electrocatalytic performance of Pd/Gr/PPy-SDBS/Ti electrode. Electrochemically reductive dechlorination with the electrode was investigated.

2. Experimental

2.1. Chemicals and materials

Experimental chemicals including hydrochloric acid (HCl), sulfuric acid (H_2SO_4 , 98%), sodium sulphate (Na_2SO_4),

sodium carbonate (Na_2CO_3), oxalic acid ($\text{H}_2\text{C}_2\text{O}_4$), isopropanol and palladium chloride (PdCl_2) powder were analytical reagent, and they were supplied by Beijing Chemical Works. Sodium dodecyl benzene sulfonate (SDBS) was guaranteed reagent and was supplied by Beijing Chemical Works. Pyrrole (Py) was chemical pure and was from Sinopharm Chemical Reagent Co., Ltd.. Gr was supplied by Chengdu Organic Chemicals Co., Ltd. 2,4,6-TCP was from AccuStandard Inc., USA. Cation-exchange membrane Nafion-324 was supplied by Sigma-Aldrich Chemical Co. Meshed Ti with aperture density of 150 PPI and line diameter of 0.10 mm was supplied by Anping Wire Screen Mesh Plant, China. All water used in the experiment was pretreated with Millipore-Q.

2.2. Electrode preparation

The meshed Ti plate substrate was pretreated by immersing in 0.3 mol L^{-1} Na_2CO_3 solution at the temperature of 363 K for 30 min, successively immersing in 0.1 mol L^{-1} oxalic acid of 373 K for 30 min to remove the surface grease and oxides. The PPy-SDBS film was electro-polymerized on the meshed Ti plate (the anode was the pretreated meshed Ti plate and the cathode was platinum foil) in the solution containing 0.1 mol L^{-1} distilled Py, 1 g L^{-1} SDBS and 0.3 mol L^{-1} sulfuric acid, with depositing current of 5 mA for 5 min [29]. Then, the Gr was added into isopropyl alcohol and dispersed under ultrasonic condition for 30 min. And the Gr/PPy-SDBS/Ti electrode was prepared by drop-casting Gr dispersion evenly on the surface of the pretreated PPy-SDBS/Ti substrate and dried horizontally in the air. Finally, by using platinum foil and Gr/PPy-SDBS/Ti electrode as anode and cathode, respectively, Pd catalyst was electrodeposited on the cathode to prepare the Pd/Gr/PPy-SDBS/Ti electrode with 22.5 mmol L^{-1} PdCl_2 solution.

2.3. Dechlorination of 2,4,6-TCP

Dechlorination experiments were operated using a two-compartment cell. The cathode was Pd/Gr/PPy-SDBS/Ti electrode and the anode was platinum foil in the dechlorination process of 2,4,6-TCP. The cell was separated with a cation-exchange membrane to avoid the dechlorination products being re-chlorinated and prevent the chloride atoms generated on the prepared electrode from transporting to the anode to form Cl_2 [30]. The anolyte was 30 mL Na_2SO_4 solution and the catholyte was 30 mL Na_2SO_4 solution containing 100 mg L^{-1} 2,4,6-TCP with stirring, and the concentration of Na_2SO_4 solution was 0.05 mol L^{-1} . H_2SO_4 was used to adjust the catholyte pH. The dechlorination current ranged from 4 mA to 7 mA and the pH value ranged from 2.1 to 2.7. The electrocatalytic reduction experiments were operated under the condition of constant current.

2.4. Analysis methods

The prepared electrodes were electrochemically characterized by cyclic voltammetry (CV) using CHI 960e electrochemical workstation. The counter electrode was platinum foil and the reference electrode was an $\text{Hg}/\text{Hg}_2\text{SO}_4$ -saturated K_2SO_4 in three-electrode system. Scanning electron microscopy (SEM),

Hitachi SU8020, Japan) was used to characterize the surface morphology of electrode. X-ray diffraction (XRD, D8 Advance, Bruker, Germany) was used to analyze the crystal structure of depositing Pd particles by using Cu-K radiation. Inductively coupled plasma-atomic emission spectrometry (ICP-AES, RIS Intrepid ER/S, Thermo Elemental, USA) was used to analyze the loading amount of Pd catalyst. X-ray photoelectron spectroscopy with Al-K radiation (XPS, ThermoFisher Scientific, ESCALAB 250, USA) was used to identify the binding energy. High performance liquid chromatography (HPLC, Waters, USA) was used to detect the concentrations of 2,4,6-TCP, intermediates and products. HPLC was consisted of Waters 1525 binary HPLC pump and 2489 UV/visible detector equipped with a Kromasil C18 reverse-phase column. The mobile phase was the mixture of 30% water and 70% methanol and the detection wavelength was 280 nm. High performance ion chromatography (HPIC, Metrohm, 883 Basic IC plus) was used to detect the concentration of Cl⁻.

2.5. Calculation of removal efficiency and current efficiency

The removal efficiency (η) was calculated with Eq. (5):

$$\eta(\%) = (C_0 - C_t) / C_0 \times 100 \quad (5)$$

where C_0 is the initial concentration of 2,4,6-TCP (mg L^{-1}), C_t is 2,4,6-TCP concentration at different electrolysis time t (mg L^{-1}).

The current efficiency (ϕ) was expressed as the percentage of electrons which were used to convert 2,4,6-TCP to 2,6-dichlorophenol(2,6-DCP), 2,4-dichlorophenol(2,4-DCP), 2-chlorophenol(2-CP) and phenol, and it could be calculated with Eq. (6):

$$\phi(\%) = [(m_1 \times n_1 - \sum(m_i \times n_i)) \times F] / (I \times t) \times 100 \quad (6)$$

where m_1 is the quantity of the converted 2,4,6-TCP (mol), n_1 is the number of electrons to convert 2,4,6-TCP to phenol ($n_1 = 6$), m_i is the quantity of the residual 2,6-DCP, 2,4-DCP and 2-CP (mol), n_i is the number of electrons to convert 2,6-DCP, 2,4-DCP and 2-CP to phenol ($n_i = 4, 4, 2$, respectively), F is the Faraday constant ($96,500 \text{ C mol}^{-1}$), I and t are dechlorination current (A) and dechlorination time (s), respectively.

3. Results and discussion

3.1. Optimization of electrode preparation

3.1.1. Effect of Gr mass concentration

With depositing current of 20 mA and depositing time of 45 min, the effect of Gr mass concentration (0.02%, 0.04%, 0.06%, 0.08% and 0.1%, respectively) was investigated. Fig. 1 shows the CV curves of Pd/Gr/PPy-SDBS/Ti electrodes prepared under different Gr concentrations. It showed that with the increasing of Gr concentration, the hydrogen adsorption peak current increased when the Gr concentration was lower than 0.04%, whereas it decreased when the Gr concentration was higher than 0.04%. The maximal value was obtained at the Gr concentration of 0.04%. The

reason was that, the loading of Gr was insufficient under low Gr concentration, which could not provide the large surface area for the deposition of Pd catalyst. When the Gr concentration was too high, the Gr adhering to the surface of the electrode stacked together or even shed from the surface. It also could not provide enough surface area for the deposition of Pd catalyst, which reduced the effective area of catalytic reaction. Therefore, it showed the low hydrogen adsorption peak current value and the low catalytic activity.

Therefore, the optimum Gr mass concentration was 0.04% for the preparation of Pd/Gr/PPy-SDBS/Ti electrode within the investigated range of research.

3.1.2. Effect of depositing current

With Gr concentration of 0.04% and electrodepositing time of 45 min, the effect of depositing current (15 mA, 20 mA, 25 mA, 30 mA and 35 mA, respectively) was investigated. Fig. 2 shows the CV curves of Pd/Gr/PPy-SDBS/Ti electrodes prepared under different depositing currents. With the increase of depositing current, the hydrogen adsorption peak current increased when the current was lower than 25 mA, whereas it decreased when the current was higher than 25 mA. The maximal value was obtained at the depositing current of 25 mA. The reason was that, the loading of Pd catalyst on the electrode was low under the low depositing current, which resulted in the low hydrogen adsorption peak current value, whereas Pd catalyst deposited on the electrode was too dense under the high depositing current and the electrode surface area decreased or Pd catalyst even shed from the surface, which also resulted in the degradation of catalytic performance.

Therefore, the optimum Pd depositing current was 25 mA for the preparation of Pd/Gr/PPy-SDBS/Ti electrode within the investigated range of research.

3.1.3. Effect of electrodepositing time

The effect of electrodepositing time was further investigated with Gr concentration of 0.04% and depositing

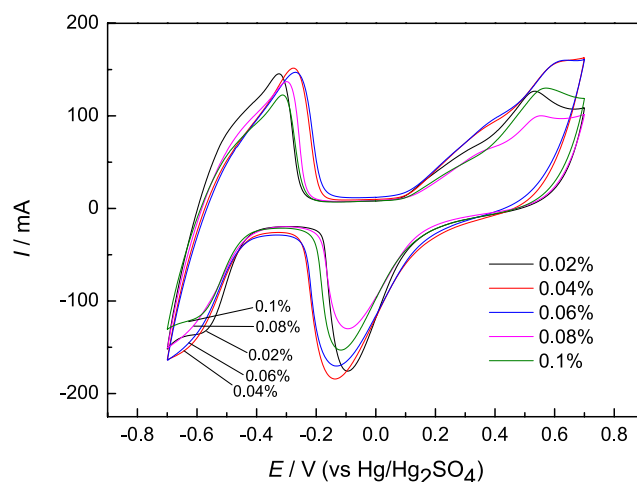


Fig. 1. CV curves of Pd/Gr/PPy-SDBS/Ti electrodes prepared under different Gr concentrations.

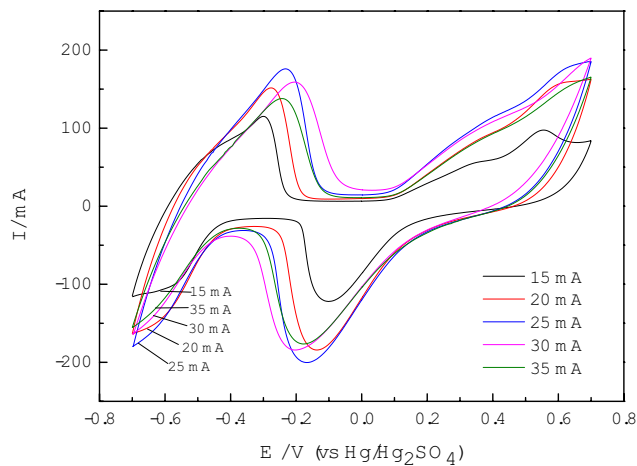


Fig. 2. CV curves of Pd/Gr/PPy-SDBS/Ti electrodes prepared under different depositing currents.

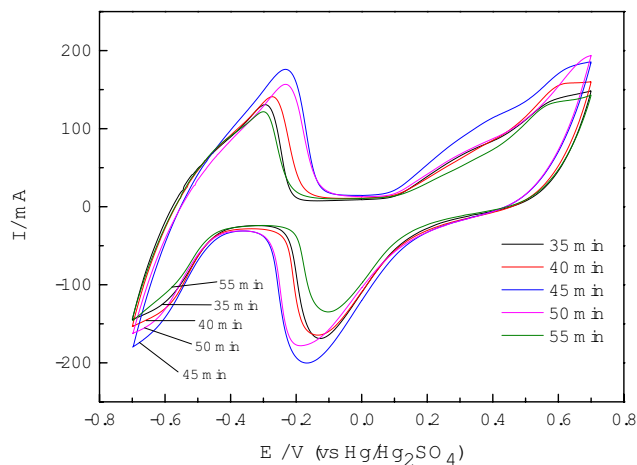


Fig. 3. CV curves of Pd/Gr/PPy-SDBS/Ti electrodes prepared under different depositing time.

current of 25 mA. Fig. 3 shows the CV curves of Pd/Gr/PPy-SDBS/Ti electrodes prepared under different depositing time (35 min, 40 min, 45 min, 50 min and 55 min, respectively). It showed that, the maximal hydrogen adsorption peak current was obtained at the depositing time of 45 min within the investigated time range. As mentioned earlier, the deposition amount of Pd catalyst and catalytic activity were both low under the short depositing time, whereas Pd catalyst deposited densely on the electrode or even shed under long depositing time and the electrode surface area decreased, which also resulted in the low catalytic activity.

Therefore, the optimum Pd electrodeposition time was 45 min for the preparation of Pd/Gr/PPy-SDBS/Ti electrode within the investigated range of research.

To sum up, the optimum depositing current, depositing time and Gr concentration were 25 mA, 45 min and 0.04%, respectively. Within the investigated range, the maximal hydrogen adsorption peak current of the prepared electrode was obtained under these optimized conditions.

3.2. Electrode characterization

3.2.1. The electrochemical characteristics of the electrodes

CV measurement of the electrodes was carried out in 0.5 mol L⁻¹ H₂SO₄ solution, and the scan rate was 50 mV s⁻¹. Fig. 4 exhibits the CV curves of the Pd/Gr/PPy-SDBS/Ti electrode. As comparison, the Pd/Ti electrode and the Pd/PPy-SDBS/Ti electrode prepared under the same conditions were also studied in the research. The curves show that the hydrogen adsorption current value of the Pd/PPy-SDBS/Ti electrode was higher than that of the Pd/Ti electrode, whereas the hydrogen adsorption current value of the Pd/Gr/PPy-SDBS/Ti electrode was much higher than that of the Pd/Ti electrode and the Pd/PPy-SDBS/Ti electrode. High hydrogen adsorption current meant the excellent electrocatalytic activity [31,32]. It indicated that the introduction of PPy-SDBS improved the catalytic performance of the electrode to some extent besides adhering to Gr effectively. To be more important, the modification of Gr increased the specific surface area of Pd catalyst, which would be more effective for electrochemically reductive dechlorination. Therefore, Pd/Gr/PPy-SDBS/Ti electrode, with higher hydrogen adsorption current value, had better potential for CPs degradation.

3.2.2. The loading amount of Pd catalyst

ICP-AES was used to analyze the loading amount of Pd catalyst. The analysis results showed that the Pd catalyst loaded on the electrode was 2.58 mg cm⁻² under the selected conditions.

3.2.3. The crystalline feature of Pd particles

XRD (shown in Fig. 5) was used to examine the crystal structure of Pd particles. It showed that five diffraction peaks appeared at 2 θ values of 40.2, 46.7, 68.2, 82.1 and 86.7, which corresponded to the (111), (200), (220), (311), and (222) planes of Pd (JCPDS 5-681), respectively [33]. The XRD results indicated that the catalyst particles with the face-centered cubic (FCC) crystal structure were successfully deposited on the electrode surface. The crystallite size of Pd particles was 16.7 nm calculated by Scherrer equation.

3.2.4. The morphology characterization of the electrodes

The surface morphologies of electrodes were studied by SEM. Fig. 6 shows the SEM images of the PPy-SDBS/Ti electrode (Fig. 6a), the Gr/PPy-SDBS/Ti electrode (Fig. 6b) and the Pd/Gr/PPy-SDBS/Ti electrode (Fig. 6c).

PPy is a kind of conductive polymer with the advantages of environmental stability and good conductivity [34,35]. Fig. 6a shows that the PPy-SDBS film covered the Ti substrate uniformly with the shape of spherical apophysis, which increased the specific surface area of the electrode in some extent. And what's more, meshed Ti with smooth surface could not support Gr directly due to its poor adhesive force and Gr would peel off the electrode. However, Gr could adhere to the surface of electrode effectively due to the introduction of the PPy-SDBS

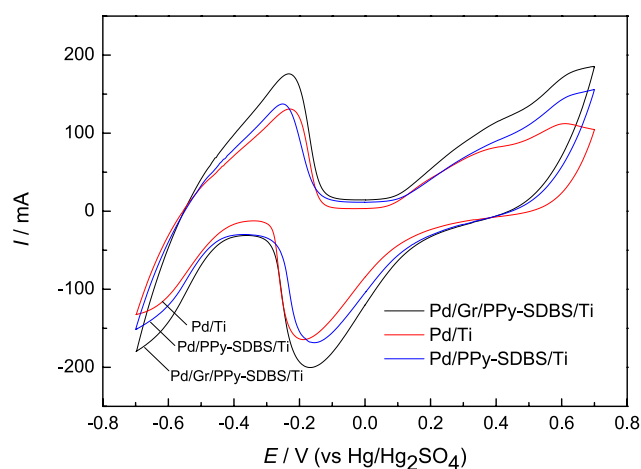


Fig. 4. CV curves of Pd/Ti electrode, Pd/PPy-SDBS/Ti electrode and Pd/Gr/PPy-SDBS/Ti electrode prepared under the selected conditions.

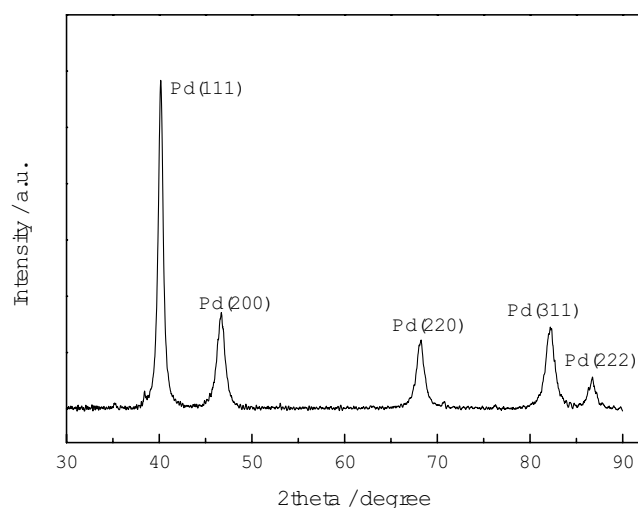


Fig. 5. XRD patterns of Pd/Gr/PPy-SDBS/Ti electrode.

film. As is shown in Fig. 6b, Gr adhered to the surface of electrode with flake-like morphology and exhibited good spatial extensibility. The structure could provide the large area for the electrodeposition of Pd microparticles. Fig. 6c shows that Pd microparticles dispersed uniformly with cauliflower-like morphology. High resolution SEM image shows that Pd microparticles presented flake-like morphology, signifying the high specific surface area and more catalytic sites of the electrode, which was favorable to reductive dechlorination.

In conclusion, PPy-SDBS film prepared by the electro-polymerization method had good stability, adhesion and favorable morphology. The addition of Gr optimized the surface structure of the electrode and improved the deposition morphology of Pd catalyst, which increased the specific surface area of Pd catalyst and supplied more reaction sites. This structure was favorable to electrochemically reductive dechlorination.

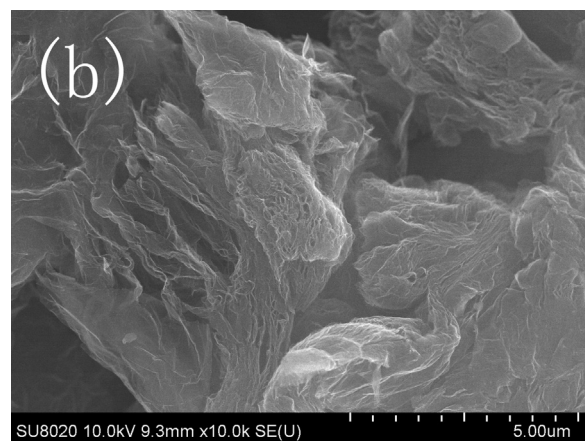
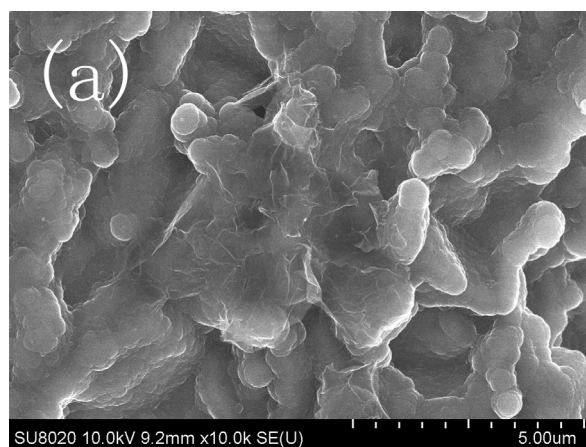


Fig. 6. SEM images of PPy-SDBS/Ti electrode (a), Gr/PPy-SDBS/Ti electrode (b) and Pd/Gr/PPy-SDBS/Ti electrode (c).

3.2.5. The composition and chemical valences of catalyst

The composition and chemical valences of catalyst at the electrode were investigated by XPS. As shown in Fig. 7, the strong peaks appeared at the binding energies of 335.6 eV and 340.8 eV can be attributed to the major spin-orbit split doublet Pd3d_{5/2} and Pd3d_{3/2} of metallic Pd⁰ [36–38], respectively. In addition, two weak peaks appeared at 338.5 eV and 343.8 eV correspond to Pd3d_{5/2} and Pd3d_{3/2} of Pd²⁺,

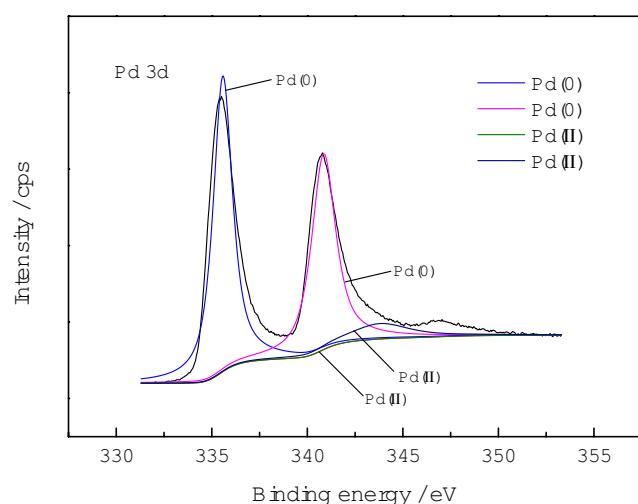


Fig. 7. XPS spectra of Pd3d of Pd/Gr/PPy-SDBS/Ti electrode.

respectively. The significantly stronger peak intensities of Pd⁰ than those of Pd²⁺ indicated that PdCl₂ was reduced successfully and Pd⁰ is the dominant component.

3.3. Electrochemically reductive dechlorination of 2,4,6-TCP

3.3.1. Effect of electrolysis current on 2,4,6-TCP dechlorination

The effects of dechlorination current on the removal efficiency and current efficiency of 2,4,6-TCP dechlorination were investigated at initial pH value of 2.5 and temperature of 298 K under different dechlorination currents (4 mA, 5 mA, 6 mA and 7 mA, respectively).

Fig. 8 shows the removal efficiencies of 2,4,6-TCP on Pd/Gr/PPy-SDBS/Ti electrode under different dechlorination currents. Dechlorination current has a significant influence on the conversion efficiency of 2,4,6-TCP on Pd/Gr/PPy-SDBS/Ti electrode in aqueous solution. When the dechlorination current was 4 mA, the conversion efficiency was low (82%) at the dechlorination time of 80 min, which was probably because the low current could not offer enough H_{ads} for the ECH. Moreover, low current corresponded to the low potential, which led to the insufficient reaction power. The conversion efficiency at current of 5 mA, 6 mA and 7 mA reached 94%, 96% and 99% within 80 min, respectively. It showed that the removal efficiency of 2,4,6-TCP improved with the increase of dechlorination current within the investigated range of research. And what's more, the conversion efficiency increased obviously when the dechlorination current rose from 4 mA to 5 mA, but slightly from 5 mA to 6 mA and 7 mA. It could be inferred that the side reaction of hydrogen evolution reaction (HER) on the electrode was intensified under the higher current, which restricted the reaction of dechlorination. Additionally, under the same dechlorination current, the removal efficiency of 2,4,6-TCP improved with the increasing of the dechlorination time.

Fig. 9 shows the current efficiencies of the dechlorination reaction under different dechlorination currents. Generally, the current efficiencies increased in the initial stage and then decreased in the later stage. The current efficiency

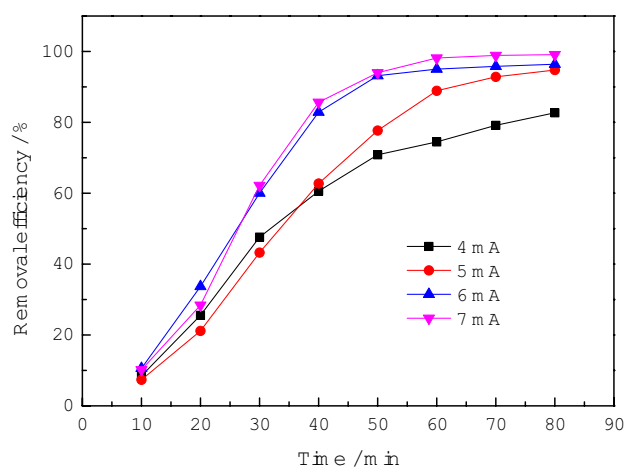


Fig. 8. Removal efficiencies of 2,4,6-TCP under different dechlorination currents. $C_{(2,4,6-TCP)0} = 100 \text{ mg L}^{-1}$, $\text{pH}_0 = 2.5$.

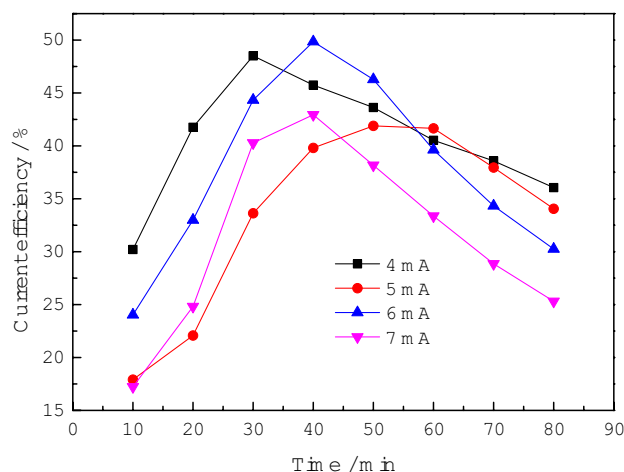


Fig. 9. Current efficiencies of the dechlorination reaction under different dechlorination currents. $C_{(2,4,6-TCP)0} = 100 \text{ mg L}^{-1}$, $\text{pH}_0 = 2.5$.

at current of 4 mA, 5 mA, 6 mA and 7 mA reached 36%, 34%, 30% and 25% within 80 min, respectively. On the basis of the mechanism of ECH, side reaction of hydrogen evolution reaction (HER) will occur inevitably. With the reaction going on, a greater proportion of H_{ads} took part in the reaction for H₂ generation, which led to the decrease of the current efficiency. And the effect of the side reaction was more significant at high current.

To have an integrative consideration of removal efficiency and current efficiency, the optimum dechlorination current was 5 mA at the initial pH value of 2.5 within the investigated range of research. At the selected current of 5 mA, the removal efficiency of 2,4,6-TCP on the Pd/Gr/PPy-SDBS/Ti electrode within 80 min reached 94%, and the current efficiency reached 34%.

3.3.2. Effect of initial pH value on 2,4,6-TCP dechlorination

The effect of initial pH value on the electrocatalytic dechlorination activity was investigated at constant current

of 5 mA within 80 min at the temperature of 298 K under different initial pH values (2.1, 2.3, 2.5 and 2.7).

Fig. 10 shows the removal efficiencies on the Pd/Gr/PPy-SDBS/Ti electrode under different initial pH values. It can be seen that the removal efficiencies increased with the increasing of the dechlorination time under the same pH value (2.1–2.7). When the initial pH value was 2.3, the complete removal was obtained within dechlorination time of 80 min. At the initial pH value of 2.1, the removal efficiency was 97% after 80 min, probably because abundant H^+ in the solution promoted the side reaction of hydrogen evolution reaction, which affected dechlorination reaction. The removal efficiency with the initial pH value of 2.5 and 2.7 were 94% and 83%, respectively. It could be attributed to the insufficiency of active hydrogen atoms for efficient dechlorination of 2,4,6-TCP.

Fig. 11 shows the current efficiencies of the dechlorination reaction under different initial pH values. Similarly, the current efficiencies increased at initial stage and then decreased with the reaction going on, revealing the same

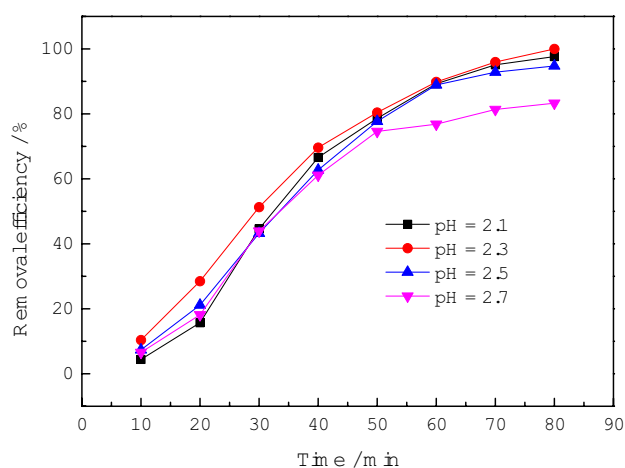


Fig. 10. Removal efficiencies of 2,4,6-TCP under different initial pH values. $C_{(2,4,6-TCP)0} = 100 \text{ mg L}^{-1}$, $I = 5 \text{ mA}$.

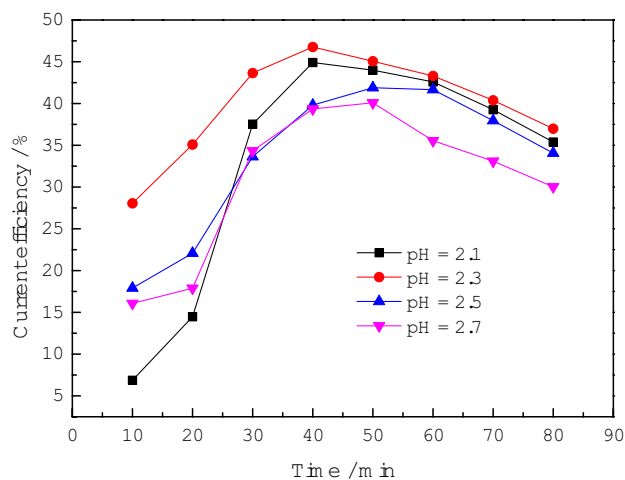


Fig. 11. Current efficiencies of the dechlorination reaction under different initial pH values. $C_{(2,4,6-TCP)0} = 100 \text{ mg L}^{-1}$, $I = 5 \text{ mA}$.

tendency with removal efficiency at the dechlorination time of 80 min under different initial pH values. The current efficiency of 36% could be obtained at dechlorination time of 80 min with the initial pH value of 2.3, which was the highest one among the investigated dechlorination pH value.

The dechlorination efficiency at constant current of 5 mA within 80 min at the initial pH value of 2.3 was also investigated, as shown in Fig. 12. Obviously, the dechlorination efficiency increased with the reaction going on, and the dechlorination efficiency of 100% was obtained after dechlorination time of 80 min when the 2,4,6-TCP was removed completely. It indicated that the organochlorines of 2,4,6-TCP were converted into inorganic chlorines completely, without generating other toxic chlorinated by-products.

To have an integrative consideration of removal efficiency, current efficiency and dechlorination efficiency, the initial pH value of 2.3 was selected for 2,4,6-TCP dechlorination on Pd/Gr/PPy-SDBS/Ti electrode. With the pH value of 2.3 and current of 5 mA, 2,4,6-TCP was removed and dechlorinated completely after dechlorination time of 80 min, and current efficiency reached 36%.

3.3.3. Effect of initial concentration of 2,4,6-TCP on dechlorination

The effects of initial concentration of 2,4,6-TCP on removal efficiency and removal amount were investigated at initial pH value of 2.3 and current of 5 mA. Figs. 13 and 14 show the removal efficiency and removal amount under different initial concentrations of 2,4,6-TCP (60 mg L^{-1} , 100 mg L^{-1} , 140 mg L^{-1} and 180 mg L^{-1}), respectively. The results showed that, the 2,4,6-TCP under four initial concentrations could be removed completely within 60 min, 80 min, 100 min and 130 min, respectively. Within the same reaction time, the higher the initial concentration, the lower the removal efficiency. However, it does not mean the low removal amount under the high initial concentration. Fig. 14 shows that the differences of the removal amount among four initial concentrations were not great at initial stage, whereas the removal amount at the same reaction time

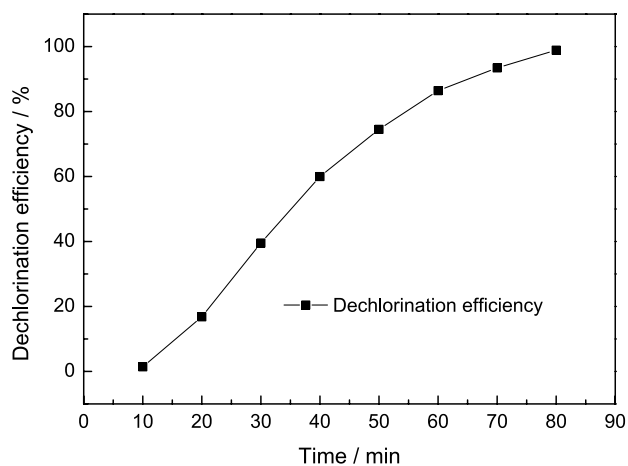


Fig. 12. Dechlorination efficiency of 2,4,6-TCP. $C_{(2,4,6-TCP)0} = 100 \text{ mg L}^{-1}$, $I = 5 \text{ mA}$, $pH_0 = 2.3$.

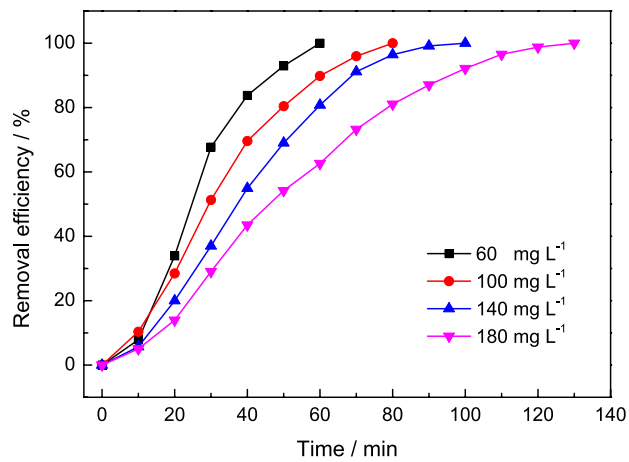


Fig. 13. Removal efficiencies of 2,4,6-TCP under different initial concentrations. $I = 5 \text{ mA}$, $\text{pH}_0 = 2.3$.

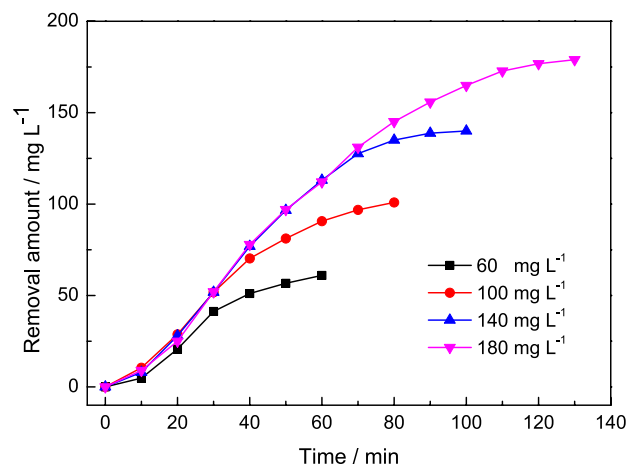


Fig. 14. Removal amounts of 2,4,6-TCP under different initial concentrations. $I = 5 \text{ mA}$, $\text{pH}_0 = 2.3$.

increased with the initial concentration in the later stage. Especially when the initial concentrations were above 100 mg L^{-1} , more than 100 mg L^{-1} of 2,4,6-TCP could be removed within 80 min. It indicated that the Pd/Gr/PPy-SDBS/Ti electrode had better potential for CPs degradation, and it was not limited to the removal capacity of 100 mg L^{-1} within 80 min.

3.3.4. The kinetics and activation energy analysis of 2,4,6-TCP dechlorination

The kinetics of 2,4,6-TCP dechlorination on the prepared Pd/Gr/PPy-SDBS/Ti electrode was investigated at the temperatures of 288 K, 298 K, 308 K and 318 K. The selected experimental conditions were as follows: electrolysis current: 5 mA, initial pH value: 2.3, initial concentration of 2,4,6-TCP: 100 mg L^{-1} .

Table 1 shows the variation of 2,4,6-TCP concentration with time at the four temperatures, where C_0 is the initial concentration of 2,4,6-TCP, C_t is the real-time con-

Table 1

Linear equations of 2,4,6-TCP dechlorination at different temperatures

Temperature	Linear equations	Coefficient of determination (R^2)
288 K	$\ln(C_0/C_t) = 0.0371 t - 0.5084$	0.9661
298 K	$\ln(C_0/C_t) = 0.0504 t - 0.6615$	0.9529
308 K	$\ln(C_0/C_t) = 0.0698 t - 0.9514$	0.9713
318 K	$\ln(C_0/C_t) = 0.0781 t - 1.1179$	0.9439

centration of 2,4,6-TCP at a certain time. Good linear fitting results were obtained between $\ln(C_0/C_t)$ and time, indicating the dechlorination reaction fitted well to the pseudo-first-order kinetics. The slopes of the fitting lines correspond to the reaction rates, and the fitting equations showed that the apparent reaction rate constant k was equal to 0.0371, 0.0504, 0.0698 and 0.0781 min^{-1} , respectively. Experimental results also showed that 2,4,6-TCP were not removed completely within 90 min at the temperature of 288 K, but removed completely within 70 min at the temperature of 318 K, which was consistent with the former analysis. The removal of 2,4,6-TCP increased with the rise of temperature, indicating that the dechlorination of 2,4,6-TCP on the Pd/Gr/PPy-SDBS/Ti electrode was endothermic reaction.

In this experiment, the Arrhenius theorem equation ($k = A \exp(-Ea/RT)$) could be used to express the effect of temperature. According to the former analysis, the effect of temperature could be formulated as $\ln(k) = -2353.471 \times T^{-1} + 4.904$ ($R^2 = 0.96$), as the fitting line shown in Fig. 15, where the slope of $\ln(k)$ versus T^{-1} equals to $-Ea/R$. Furthermore, the calculation result showed that the apparent activation energy was 19.6 kJ mol^{-1} , which indicated the dechlorination reaction was dominated by interfacial chemical reaction as well as diffusion [29].

3.3.5. Product analysis

The dechlorination products of 100 mg L^{-1} 2,4,6-TCP were analyzed under the dechlorination conditions of current of 5 mA within 80 min at initial pH value of 2.3.

Fig. 16 indicates that 2,4,6-TCP was degraded gradually in the entire process and removed completely at 80 min. The intermediate products of 2,4,6-TCP dechlorination included 2-CP, 2,6-DCP, 2,4-DCP and phenol. The quantities of the generated CPs (2-CP, 2,6-DCP and 2,4-DCP) increased at initial stage, and then decreased to 0. It was because the generation rate of the intermediate products was higher than the degradation rate at initial stage. With the concentration of 2,4,6-TCP decreasing, the generation rate decreased and was lower than the degradation rate of CPs. The maximum concentration of 2-CP reached 1.83 mg L^{-1} after the dechlorination reaction of 40 min, whereas the 4-CP was barely detected in the experiment, which indicates that the reactivity of *para*-chlorine is higher than that of *ortho*-chlorine due to the steric hindrance resulting from the hydroxyl group. In addition, the concentration of 2,4-DCP was lower than that of 2,6-DCP in the dechlorination process, which also means *para*-chlorine could be replaced easier than *ortho*-chlorine.

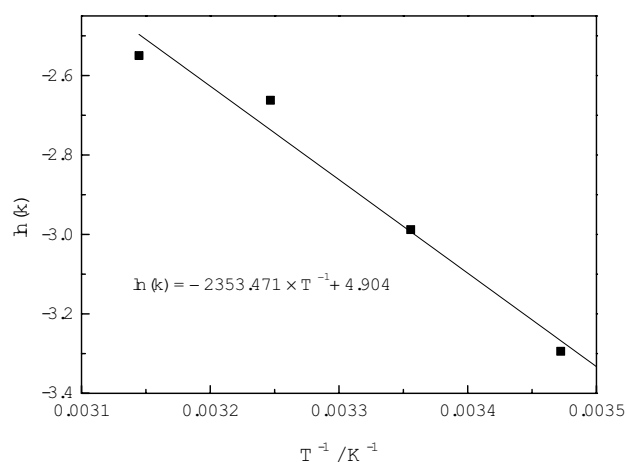


Fig. 15. Arrhenius plot of $\ln(k)$ and T^{-1} of 2,4,6-TCP dechlorination on Pd/Gr/PPy-SDBS/Ti electrode.

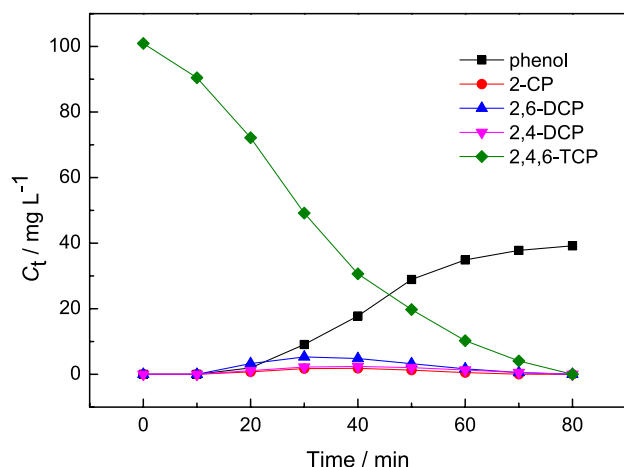


Fig. 16. Concentration variation of 2,4,6-TCP and intermediate products. $C_{(2,4,6\text{-TCP})0} = 100 \text{ mg L}^{-1}$, $I = 5 \text{ mA}$, $\text{pH}_0 = 2.3$.

Furthermore, the concentration of phenol increased during the whole dechlorination process, and the dechlorination product of 2,4,6-TCP detected by HPLC after reaction time of 80 min was phenol. However, it was calculated that the molar ratio of phenol to 2,4,6-TCP at the end of electrolysis was 81%. Thus, it implied that some phenol could be further reduced to other dechlorination products with time extending, though there were no other new peaks detected under selected chromatographic condition. The main substance generated from phenol reduction was cyclohexanone [22].

It should be pointed out that no intermediate products were detected in the first 10 min when the concentration of 2,4,6-TCP decreased slightly, and it was probably because the amount of intermediate products generated at initial stage was small and they were absorbed on the electrode surface without diffusing into the solution. Moreover, it was attributed to the adsorption of 2,4,6-TCP on the electrode surface from the solution without being degraded yet. We conducted the control experiment under the same conditions but without electrical current to assess the contribution of adsorption. The result showed that the adsorp-

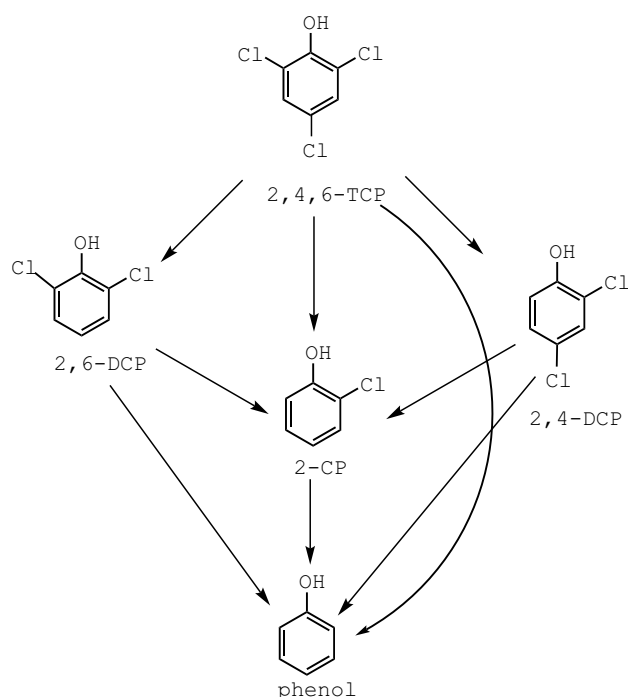


Fig. 17. The electrocatalytic degradation pathways of 2,4,6-TCP.

tion capacity in the first 10 min was about 2% of the total amount of 2,4,6-TCP.

3.3.6. Electrocatalytic degradation pathways of 2,4,6-TCP

By the analysis of intermediates and products, the electrocatalytic degradation pathways of 2,4,6-TCP are as following: as the intermediate products were not detected in the first 10 min, but detected at 20 min, it could be inferred that one or two chlorines were replaced by the active hydrogen to generate 2,4-DCP, 2,6-DCP and 2-CP. In addition, 2,4-DCP, 2,6-DCP and 2-CP were not detected except phenol at dechlorination time of 80 min when 2,4,6-TCP was removed completely. It indicated that three chlorines could be replaced simultaneously to generate phenol directly. According to the relevant literature [39,40], there were two pathways of 2,4-DCP degradation, *para*-chlorine was replaced first by the active hydrogen to generate 2-CP and then 2-CP was dechlorinated to phenol, or *ortho*-chlorine and *para*-chlorine were replaced simultaneously to generate phenol directly. Similarly, there were two pathways of 2,6-DCP degradation, one *ortho*-chlorine was replaced to generate 2-CP and then 2-CP was dechlorinated to phenol, or two *ortho*-chlorines were replaced simultaneously to generate phenol directly.

In summary, according to the former analysis, the electrocatalytic degradation pathways of 2,4,6-TCP are illustrated in Fig. 17.

3.3.7. Stability of Pd/Gr/PPy-SDBS/Ti electrode

The stability of the electrode was tested by repeating the experiment for 10 times with the same electrode. The

experiment showed that, after 10 times of dechlorination, the removal efficiency of 2,4,6-TCP could still reach 98%, which indicated that the Pd/Gr/PPy-SDBS/Ti electrode had the good stability.

4. Conclusions

After the PPy-SDBS film was polymerized on the surface of meshed Ti plate, Pd/Gr/PPy-SDBS/Ti electrode was successfully prepared by the simple drop-casting/electrodeposition process. The introduction of Gr optimized the surface structure of the electrode and improved the catalytic activity. Within the investigated range, the maximal hydrogen adsorption peak current of the electrode prepared under the selected conditions was obtained, which was much higher than that of Pd/Ti electrode prepared without modification. The dechlorination property of the prepared Pd/Gr/PPy-SDBS/Ti electrode was investigated with the dechlorination experiment of 2,4,6-TCP. To have an integrative consideration of removal efficiency, current efficiency and dechlorination efficiency, the optimum dechlorination current and initial pH value within the investigated range were 5 mA and 2.3, respectively. Under the selected conditions, 100 mg L⁻¹ 2,4,6-TCP in aqueous solution could be removed and dechlorinated completely within 80 min, and the current efficiency reached 36%. Dechlorination experiments under the high initial concentrations indicated that the removal capacity within 80 min was more than 100 mg L⁻¹. The intermediate products included phenol, 2-CP, 2,6-DCP and 2,4-DCP, and the main final product was phenol. The reaction fitted well to the pseudo-first-order kinetics. The apparent activation energy of 2,4,6-TCP dechlorination on the electrode was 19.6 kJ mol⁻¹. The prepared Pd/Gr/PPy-SDBS/Ti electrode with high electrocatalytic activity may provide a promising approach for electrocatalytic degradation of CPs.

Acknowledgements

This study was funded by National Natural Science Foundation of China (51478014, 51278006) and Cultivation Fund for Beijing New Century Hundred, Thousand and Ten Thousand Talents Project.

References

- [1] O. Scialdone, A. Galia, L. Gurreri, S. Randazzo, Electrochemical abatement of chloroethanes in water: Reduction, oxidation and combined processes, *Electrochim. Acta.*, 55 (2010) 701–708.
- [2] N. Yang, J. Cui, L. Zhang, W. Xiao, A.N. Alshawabkeh, X. Mao, Iron electrolysis-assisted peroxydisulfate chemical oxidation for the remediation of chlorophenol-contaminated groundwater, *J. Chem. Technol. Biotechnol.*, 91 (2016) 938–947.
- [3] S.M. Khor, C.E. Seng, P.E. Lim, S.L. Ng, A. Sujari, Activated rice husk-based adsorbents for chlorophenol removal and their bioregeneration, *Desal. Water Treat.*, 57 (2016) 10349–10360.
- [4] Proposition 65, Office of Environmental Health Hazard, EPA, State of California, USA, 2005.
- [5] S.K. Garg, M. Tripathi, S.K. Singh, A. Singh, Pentachlorophenol dechlorination and simultaneous Cr⁶⁺ reduction by *Pseudomonas putida* SKG-1 MTCC (10510): characterization of PCP dechlorination products, bacterial structure, and functional groups, *Environ. Sci. Pollut. Res.*, 20 (2013) 2288–2304.
- [6] L. Zhang, B. Zhang, T. Wu, D. Sun, Y. Li, Adsorption behavior and mechanism of chlorophenols onto organoclays in aqueous solution, *Colloids Surf. A.*, 484 (2015) 118–129.
- [7] E.M. Soliman, H.M. Albishri, H.M. Marwani, M.G. Batterjee, Removal of 2-chlorophenol from aqueous solutions using activated carbon-impregnated Fe(III), *Desal. Water Treat.*, 51 (2013) 6655–6662.
- [8] Y.A. Mustafa, A.H. Shihab, Removal of 4-chlorophenol from wastewater using a pilot-scale advanced oxidation process, *Desal. Water Treat.*, 51 (2013) 6663–6675.
- [9] D.M. Angelucci, M.C. Tomei, Pentachlorophenol aerobic removal in a sequential reactor: start-up procedure and kinetic study, *Environ. Technol.*, 36 (2015) 327–335.
- [10] L. Beristain-Montiel, S. Martinez-Hernandez, C.F. de Maria, F. Ramirez-Vives, Dynamics of a microbial community exposed to several concentrations of 2-chlorophenol in an anaerobic sequencing batch reactor, *Environ. Technol.*, 36 (2015) 1776–1784.
- [11] O. Lugaesi, J.V. Perales-Rondón, A. Minguzzi, J. Solla-Gullón, S. Rondinini, J.M. Feliu, C.M. Sánchez-Sánchez, Rapid screening of silver nanoparticles for the catalytic degradation of chlorinated pollutants in water, *Appl. Catal. B.*, 163 (2015) 554–563.
- [12] C. Ma, H. Ma, Y. Xu, Y. Chu, F. Zhao, The roughened silver-palladium cathode for electrocatalytic reductive dechlorination of 2,4-dichlorophenoxyacetic acid, *Electrochem. Commun.*, 11 (2009) 2133–2136.
- [13] C. Cui, X. Quan, H. Yu, Y. Han, Electrocatalytic hydrodehalogenation of pentachlorophenol at palladized multiwalled carbon nanotubes electrode, *Appl. Catal. B.*, 80 (2008) 122–128.
- [14] Y. Xu, Q. Cai, H. Ma, Y. He, H. Zhang, C. Ma, Optimisation of electrocatalytic dechlorination of 2,4-dichlorophenoxyacetic acid on a roughened silver-palladium cathode, *Electrochim. Acta.*, 96 (2013) 90–96.
- [15] I.F. Cheng, Q. Fernando, N. Korte, Electrochemical dechlorination of 4-chlorophenol to phenol, *Environ. Sci. Technol.*, 31 (1997) 1074–1078.
- [16] C. Sun, S.A. Baig, Z. Lou, J. Zhu, Z. Wang, X. Li, J. Wu, Y. Zhang, X. Xu, Electrocatalytic dechlorination of 2,4-dichlorophenoxyacetic acid using nanosized titanium nitride doped palladium/nickel foam electrodes in aqueous solutions, *Appl. Catal. B.*, 158–159 (2014) 38–47.
- [17] B. Yang, G. Yu, D. Shuai, Electrocatalytic hydrodechlorination of 4-chlorobiphenyl in aqueous solution using palladized nickel foam cathode, *Chemosphere*, 67 (2007) 1361–1367.
- [18] X. Mao, A. Ciblak, M. Amiri, A.N. Alshawabkeh, Redox control for electrochemical dechlorination of trichloroethylene in bicarbonate aqueous media, *Environ. Sci. Technol.*, 45 (2011) 6517–6523.
- [19] J. Zhang, Z. Cao, Y. Chi, L. Xie, L. Lin, Preparation and electrocatalytic dechlorination performance of Pd/Ti electrode, *Desalin. Water Treat.*, 54 (2015) 2692–2699.
- [20] W. Xie, S. Yuan, X. Mao, W. Hu, P. Liao, M. Tong, A.N. Alshawabkeh, Electrocatalytic activity of Pd-loaded Ti/TiO₂ nanotubes cathode for TCE reduction in groundwater, *Water Res.*, 47 (2013) 3573–3582.
- [21] Y. Wu, C. Hsu, T.M. Chang, M. Sone, C. Hu, Preparation and characterization of palladium-hydride-coated titanium as a reference electrode for the supercritical carbon dioxide emulsion electrochemical system, *Electrochim. Acta.*, 155 (2015) 209–216.
- [22] Z. Sun, X. Wei, Y. Han, S. Tong, X. Hu, Complete dechlorination of 2,4-dichlorophenol in aqueous solution on palladium/polymeric pyrrole-cetyl trimethyl ammonium bromide/foam-nickel composite electrode, *J. Hazard. Mater.*, 244–245 (2013) 287–294.
- [23] Z. He, J. Sun, J. Wei, Q. Wang, C. Huang, J. Chen, S. Song, Effect of silver or copper middle layer on the performance of palladium modified nickel foam electrodes in the 2-chlorobiphenyl dechlorination, *J. Hazard. Mater.*, 250–251 (2013) 181–189.
- [24] J. Li, H. Liu, X. Cheng, Y. Xin, W. Xu, Z. Ma, J. Ma, N. Ren, Q. Li, Stability of palladium-polypyrrole-foam nickel electrode and its electrocatalytic hydrodechlorination for dichlorophenol isomers, *Ind. Eng. Chem. Res.*, 51 (2012) 15557–15563.

- [25] K.S. Novoselov, V.I. Fal'ko, L. Colombo, P.R. Gellert, M.G. Schwab, K. Kim, A roadmap for graphene, *Nature*, 490 (2012) 192–200.
- [26] H. Gao, L. Song, W. Guo, L. Huang, D. Yang, F. Wang, Y. Zuo, X. Fan, Z. Liu, W. Gao, R. Vajtai, K. Hackenberg, P.M. Ajayan, A simple method to synthesize continuous large area nitrogen-doped graphene, *Carbon*, 50 (2012) 4476–4482.
- [27] X. Li, Y. Zhu, W. Cai, M. Borysiak, B. Han, D. Chen, R.D. Piner, L. Colombo, R.S. Ruoff, Transfer of large-area graphene films for high-performance transparent conductive electrodes, *Nano Lett.*, 9 (2009) 4359–4363.
- [28] A. Bianco, H.M. Cheng, T. Enoki, Y. Gogotsi, R.H. Hurt, N. Koratkar, T. Kyotani, M. Monthieux, R.P. Chong, J. Tascon, All in the graphene family - a recommended nomenclature for two-dimensional carbon materials, *Carbon*, 65 (2013) 1–6.
- [29] Z. Sun, X. Wei, H. Zhang, X. Hu, Dechlorination of pentachlorophenol (PCP) in aqueous solution on novel Pd-loaded electrode modified with PPy-SDBS composite film, *Environ. Sci. Pollut. Res.*, 22 (2015) 3828–3837.
- [30] Z. Sun, H. Ge, X. Hu, Y. Peng, Preparation of foam-nickel composite electrode and its application to 2,4-dichlorophenol dechlorination in aqueous solution, *Sep. Purif. Technol.*, 72 (2010) 133–139.
- [31] J. Zhang, M. Huang, H. Ma, F. Tian, W. Pan, S. Chen, High catalytic activity of nanostructured Pd thin films electrochemically deposited on polycrystalline Pt and Au substrates towards electro-oxidation of methanol, *Electrochem. Commun.*, 9 (2007) 1298–1304.
- [32] X. Hu, H. Ge, B. Li, Z. Sun, Preparation and characterization of codeposited palladium-nickel/titanium electrodes and palladium-nickel/polymeric pyrrole film/titanium electrodes, *Chem. Eng. Technol.*, 31 (2008) 1396–1401.
- [33] Y. Zhao, L. Zhan, J. Tian, S. Nie, Z. Ning, N-doped amorphous carbon supported Pd catalysts for methanol electrocatalytic oxidation, *Acta Phys. Chim. Sin.*, 27 (2011) 91–96.
- [34] S.H. Hosseini, A.J. Abadi, Preparation of magnetic and conductive graphite nanoflakes/Fe₃O₄ nanoparticles/polypyrrole nanocomposites, *Synth. React. Inorg. M.*, 45 (2015) 591–596.
- [35] Q. Yang, Z. Hou, T. Huang, Self-assembled polypyrrole film by interfacial polymerization for supercapacitor applications, *J. Appl. Polym. Sci.*, (2015) 41615.
- [36] G. Fu, K. Wu, J. Lin, Y. Tang, Y. Chen, Y. Zhou, T. Lu, One-pot water-based synthesis of Pt-Pd alloy nanoflowers and their superior electrocatalytic activity for the oxygen reduction reaction and remarkable methanol-tolerant ability in acid media, *J. Phys. Chem. C.*, 117 (2013) 9826–9834.
- [37] C. Hsieh, Y. Liu, Y. Cheng, W. Chen, Microwave-assisted synthesis and pulse electrodeposition of palladium nanocatalysts on carbon nanotube-based electrodes, *Electrochim. Acta.*, 56 (2011) 6336–6344.
- [38] V. Lim, E.T. Kang, K.G. Neoh, Electroless plating of palladium and copper on polypyrrole films, *Synth. Met.*, 123 (2001) 107–115.
- [39] E.J. Shin, M.A. Keane, Detoxification of dichlorophenols by catalytic hydrodechlorination using a nickel/silica catalyst, *Chem. Eng. Sci.*, 54 (1999) 1109–1120.
- [40] X. Wang, M. Zhu, H. Liu, J. Ma, F. Li, Modification of Pd-Fe nanoparticles for catalytic dechlorination of 2,4-dichlorophenol, *Sci. Total Environ.*, 449 (2013) 157–167.